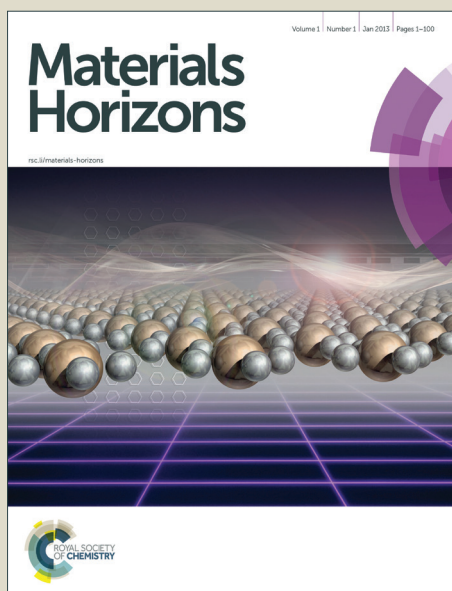


# Materials Horizons

Accepted Manuscript



This is an *Accepted Manuscript*, which has been through the Royal Society of Chemistry peer review process and has been accepted for publication.

*Accepted Manuscripts* are published online shortly after acceptance, before technical editing, formatting and proof reading. Using this free service, authors can make their results available to the community, in citable form, before we publish the edited article. We will replace this *Accepted Manuscript* with the edited and formatted *Advance Article* as soon as it is available.

You can find more information about *Accepted Manuscripts* in the [Information for Authors](#).

Please note that technical editing may introduce minor changes to the text and/or graphics, which may alter content. The journal's standard [Terms & Conditions](#) and the [Ethical guidelines](#) still apply. In no event shall the Royal Society of Chemistry be held responsible for any errors or omissions in this *Accepted Manuscript* or any consequences arising from the use of any information it contains.

## Conceptual insights

### Stem Cell-Compatible Eumelanin Biointerface by Chemically-Controlled Solid State Polymerization

Alessandro Pezzella, Mario Barra, Anna Musto, Angelica Navarra, Michela Alfè, Paola Manini, Silvia Parisi, Antonio Cassinese, Valeria Criscuolo, Marco d'Ischia

This work discloses a pioneering eumelanin thin film as operational platform for stem cell growth and differentiation. Key elements of the technology allowing exploitation of the natural pigment as a bioinspired and biocompatible semiconductor thin film are the solvent free fabrication protocol, the mild reaction conditions and the chemical control on polymer structure. The resulting films feature remarkable adhesion properties responsible for the film stability to water and the consequent reversibility in water induced eumelanin electrical properties switch. Further, the solid state procedure resulted in the retention of the pigment backbone integrity, avoiding oxidative ring fission and associated loss of aromatic stacking units. The convergence of all these elements does provide the ground for the actual exploitation of eumelanin based devices in organic electronics.

Cite this: DOI: 10.1039/c0xx00000x

www.rsc.org/xxxxxx

ARTICLE TYPE

# Stem Cell-Compatible Eumelanin Biointerface by Chemically-Controlled Solid State Polymerization†

Alessandro Pezzella,<sup>\*a</sup> Mario Barra,<sup>b</sup> Anna Musto,<sup>c,d</sup> Angelica Navarra,<sup>c,d</sup> Michela Alfè,<sup>e</sup> Paola Manini,<sup>a</sup> Silvia Parisi,<sup>c,d</sup> Antonio Cassinese,<sup>b</sup> Valeria Criscuolo,<sup>a</sup> Marco d'Ischia<sup>a</sup>

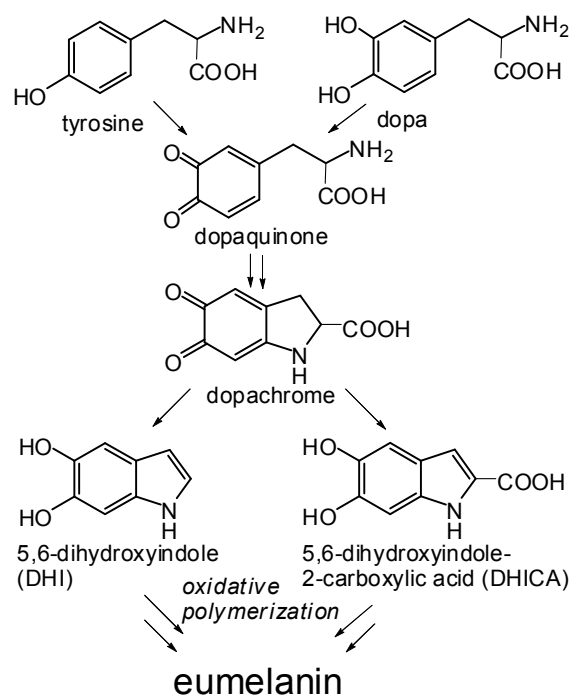
<sup>5</sup> Received (in XXX, XXX) Xth XXXXXXXXX 20XX, Accepted Xth XXXXXXXXX 20XX

DOI: 10.1039/b000000x

Relying on the water-dependent hybrid conductor properties of eumelanin biopolymers, a structurally-controlled melanin thin film that can be reversibly switched-on and off by hydration/dehydration cycles and that can be used as a biocompatible platform for stem cell growth and differentiation up to 11 days is reported. Key feature of the new eumelanin-based bioelectronic interface is a remarkable structural regularity and integrity, as the result of ad hoc fabrication protocol involving ammonia-induced solid state polymerization (AISSP) technology of a 5,6-dihydroxyindole thin film. The AISSP technology is operationally simple and versatile, enabling the preparation of device-quality thin films (AFM and MALDI-MS evidence) on various substrates with efficient chemical control over molecular complexity. Overall these results pave the way to the implementation of tailored eumelanin thin films for bioelectronics, e.g. for organic electrochemical transistors (OECT).

## Introduction

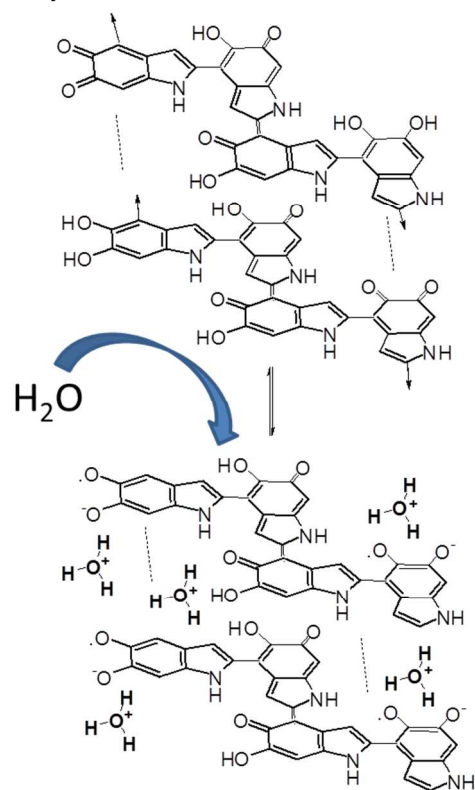
The implementation of organic interfaces for electrical stimulation of cell-tissue constructs is a central goal in the rapidly expanding fields of bioelectronics and nanomedicine, and is contingent upon the development of biocompatible, easily accessible and tailored organic semiconductors. Among the various Nature-inspired materials that hold promise for the design of bioelectronic interfaces, eumelanins, the black insoluble photoprotective biopolymers of human skin and eyes,<sup>1-3</sup> occupy a prominent position. Both natural and synthetic eumelanins display peculiar optoelectronic properties,<sup>4, 5</sup> which are exemplified in a water-dependent semiconductor-like behavior,<sup>6-8</sup> broad band absorption,<sup>9, 10</sup> permanent paramagnetism<sup>11, 12</sup> and efficient non-radiative UV-dissipation.<sup>13, 14</sup> These features were originally attributed to an amorphous semiconductor structure<sup>6, 9</sup> but, more recently, they have been explained in terms of a chemical disorder model<sup>15</sup> as integrated to include a dynamic component of reversible intermolecular interactions perturbing  $\pi$ -electron systems.<sup>10, 16</sup> Structural disorder in eumelanins derives from their complex biosynthetic origin from the tyrosinase-catalyzed oxidation of tyrosine and/or dopa (Scheme 1). In this process copolymerization of the various intermediates produced from dopa to 5,6-dihydroxyindole (DHI) metabolites, and post-synthetic oxidative breakdown of monomer units,<sup>3</sup> do generate an entire array of chemically different species.



<sup>45</sup> **Scheme 1.** Schematic view of eumelanin synthesis from tyrosine or dopa. Representative intermediates in the process are highlighted.

In line with the dynamic chemical disorder model, humidity-dependent electrical properties of eumelanins have been attributed to a peculiar electronic-ionic hybrid conductor behavior,<sup>7</sup> in which thermodynamically-favorable, water-driven

redox equilibria between catechol and quinone species would generate semiquinone moieties<sup>17</sup> doping electrons and protons into the system.



5

**Scheme 2.** Simplified illustration of the water-dependent self-doping mechanism of DHI melanin based on the previously suggested water driven comproportionation equilibrium between o-diphenol and o-quinone units leading to an increased proportion of semiquinone radical anions (electrons) and hydronium ions (protons).

In the framework of a basic model identifying eumelanin in its solid-state form as an amorphous semiconductor, it was suggested that the eumelanin dielectric constant increases in presence of water, thus lowering the activation energy which rules the charge carrier hopping phenomenon.<sup>6,7,18</sup>

This effect was also considered to justify the occurrence of electrical switchings in eumelanin pellets and films, with the conductivity values changing by many orders of magnitude when the applied electrical field exceeds a threshold value.<sup>6,19</sup> More recently, an alternative model was proposed pointing out that eumelanin hydration conditions modify the comproportionation equilibrium, in such a way that the densities of both electrons and protons are considerably increased into the system, thus justifying the observed electrical conductivity change.<sup>7</sup>

Although further test are required, it may be conjectured that the role of water is to mediate the formation of hydrogen bonds between parallel sheets of stacked oligomers favoring dynamic equilibration of tautomeric molecular components and charge movement across the film. Water may also affect local dielectric constant favoring ionization of acid groups within eumelanin constituents. (Scheme 2)

30

Despite a burst of interest in the use of synthetic eumelanins and related biopolymers<sup>20-22</sup> for organic electronics and bioelectronics,<sup>1, 23-26</sup> the implementation of competitive eumelanin-based technology has so far been hindered by several drawbacks. These latter include a complete insolubility in all solvents, preventing development of standardized and reproducible synthetic procedures, and the lack of a solid conceptual frame of structure-property-function relationships. In consequence, eumelanin-based thin films are commonly prepared from structurally ill-defined commercially available materials<sup>23, 26</sup> or by prolonged alkaline oxidation of dopa<sup>27</sup> or dopamine,<sup>22</sup> causing severe alkali-induced post-synthetic degradation adding to the intrinsic structural disorder.<sup>20</sup> Although the impact of the high molecular heterogeneity on the electrical performances of eumelanins has not been systematically assessed, several critical drawbacks can be anticipated as, for example, the lack of well-defined HOMO-LUMO gaps. A heterogeneous composition in terms of structural units is obviously detrimental for effective tailoring of chemical properties and for film quality, an important requisite for cell growth. As a matter of fact, the usual translation of structure-property relationships into rational design rules and effective chemical manipulation strategies to engineer high quality materials has remained a most difficult task in the case of eumelanins.

In this paper, we report remarkable advancements in eumelanin chemistry that surmount most of those issues. Disclosed herein are: a) an original strategy that allowed to overcome most of the drawbacks limiting competitiveness in eumelanin-based technology and leading for the first time to high quality thin films with efficient chemical control on structural heterogeneity and complexity; b) the ability of the new bio-inspired material to be reversibly switched on and off by controlled hydration-dehydration steps; and c) the efficient growth and differentiation of stem cells seeded on the novel eumelanin thin films.

## Eumelanin Thin Film Fabrication.

Typical eumelanin thin film fabrication protocols involve direct deposition of the pigment. Because of the unfavorable properties of eumelanin (chiefly insolubility in any solvent<sup>3</sup>), film fabrication requires a pretreatment of dopa or tyrosine derived eumelanin to gain at least partial solubilization.<sup>28</sup> The most commonly adopted aqueous alkaline treatment results in serious pigment backbone modification associated with aromatic ring fission<sup>29</sup> and consequent loss of chemically defined properties with increase of chemical disorder.<sup>20</sup>

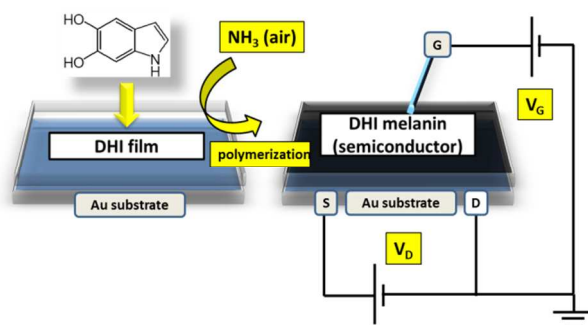
Such scenario appears unwanted in order to achieve chemically defined films, a fundamental goal because of the impact of chemical structure on functional properties.<sup>30</sup> Structural control from molecular scale level, jointly with the knowledge of chemical physical properties of the film material, are thus mandatory for rational design of eumelanin-based devices.

The approach we devised allows turning the intractable nature of eumelanin into advantages.

The rationale inspiring this approach was the use of DHI as the eumelanin precursor in the place of commonly used dopa or dopamine, for the following reasons: 1) DHI is soluble in organic solvents and is the ultimate monomer precursor in the pathways of natural and synthetic eumelanins, ensuring the generation of homopolymers rather than copolymers of various intermediates, as in the case of dopa and dopamine melanins,<sup>3,11,21</sup>; 2) the mode of polymerization of DHI and its dimers and oligomers,<sup>17,31-35</sup> the mechanisms of aggregation underlying particle growth,<sup>36</sup> and

the optical and free radical properties of DHI melanin<sup>11, 16</sup> have all been clarified in detail; 3) the electrical properties of DHI melanin suspensions have been characterized using an organic-electrochemical transistor;<sup>37</sup> 4) DHI melanin can be used to prepare thin films by a variety of methodologies, although their morphological properties are not always of high quality.<sup>38, 39</sup>

The manifold problems associated with the limited processability of insoluble eumelanins were then overcome by rational development of a procedure, referred to as ammonia-induced solid state polymerization (AISSP), which is based on the uniform deposition by spin coating of the soluble DHI monomer as highly homogeneous thin films, followed by solid state polymerization induced by exposure to gaseous ammonia in air-equilibrated atmosphere (Scheme 3)



**Scheme 3.** Schematic illustration of the AISSP procedure for DHI melanin film deposition and the FET device set up for the determination of electrical properties of the eumelanin film.

Film fabrication on suitable quartz substrates allowed to easily follow the polymerization process by UV-Vis spectroscopy observing the spectra evolution with time.

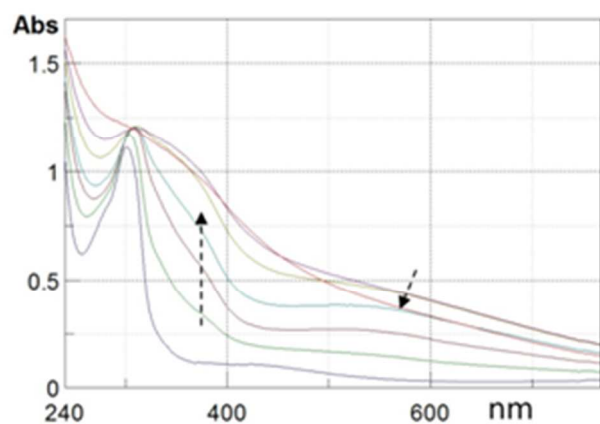


**Figure 1.** UV-vis profiles of DHI thin film under AISSP. Plots are taken at 5; 15; 30; 45; 60; 180 min after exposition to polymerization inducing atmosphere. Arrows denote evolution. UV-vis profile of DHI film (bottom line) is also reported. See Figure S1 of SI for corresponding images of the films on quartz.

In Figure 1 the film absorption spectra are reported at several times after AISSP was started. Here, the spectrum of the DHI film it is also reported for comparison. From the absorption profile at 60 min reaction time, it is clearly evident how the DHI

spectrum is completely evolved into the typical eumelanin profile.<sup>10, 16, 28</sup> Moreover, it is noteworthy the clear occurrence of the melanochromic intermediate phase, characterized by a broad, but distinctive, maximum around 540 nm<sup>40</sup> in the UV-vis plots in the range 10 - 30 min.

SEM images were also taken in order to check the film compactness and the quality of the adhesion on the substrates. These images (see Figure S2 of SI) demonstrate definitely that eumelanin films obtained by the AISSP procedure are structurally compact, being able to homogeneously cover the substrate surface.

More insights about the morphology of the eumelanin films were gained, by acquiring AFM images on different length scales, going from 2  $\mu\text{m}$  \* 2  $\mu\text{m}$  to 30  $\mu\text{m}$  \* 30  $\mu\text{m}$  (see Figure 2 and Figure S3 of SI). From the AFM images, it comes clear that the film surface is characterized by a very smooth matrix where the only specific morphological feature is the presence of some columnar structures having heights of few nm. On a 2  $\mu\text{m}$  \* 2  $\mu\text{m}$  scale, the average roughness results to be lower than 0.3 nm, while it increases up to about 1nm, when larger scales are considered.

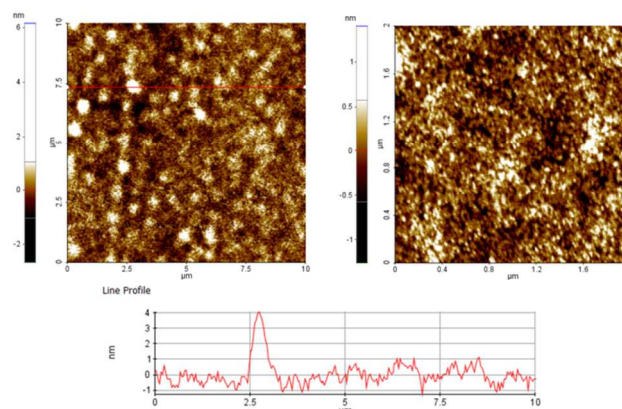


**Figure 2.** AFM topographical maps on different scales of a DHI melanin thin film grown by AISSP (a, 2 \* 2 $\mu\text{m}$ , b, 10 \* 10 $\mu\text{m}$ ) and (c) Height profile caught from the red line on map (red line).

The chemical nature of the DHI melanin films obtained by the AISSP methodology was investigated by matrix-assisted laser desorption ionization (MALDI) mass spectrometry in comparison with a dopa melanin sample, prepared by auto-oxidation in alkaline medium according to a reported protocol (Figure 3).<sup>7</sup>

MALDI-MS data allowed to appreciate several important chemical and technological advances associated with the AISSP technology. From the chemical viewpoint, when compared with representative films obtained by deposition of preformed eumelanins, such as tyrosinase-catalyzed DHI melanin and autooxidative dopa melanin, AISSP DHI films exhibit greater structural integrity, as evidenced by the regular clusters of peaks centered around the expected pseudomolecular ion peak, and a limited degree of polymerization (highest oligomer detected at the hexamer-septamer stage, to be compared with the 30-mer identified in the polymerization mixture of DHI).<sup>35</sup>

Main structural components accounting for the mass spectrum of the DHI melanin produced by AISSP are illustrated Figure S3 of SI.

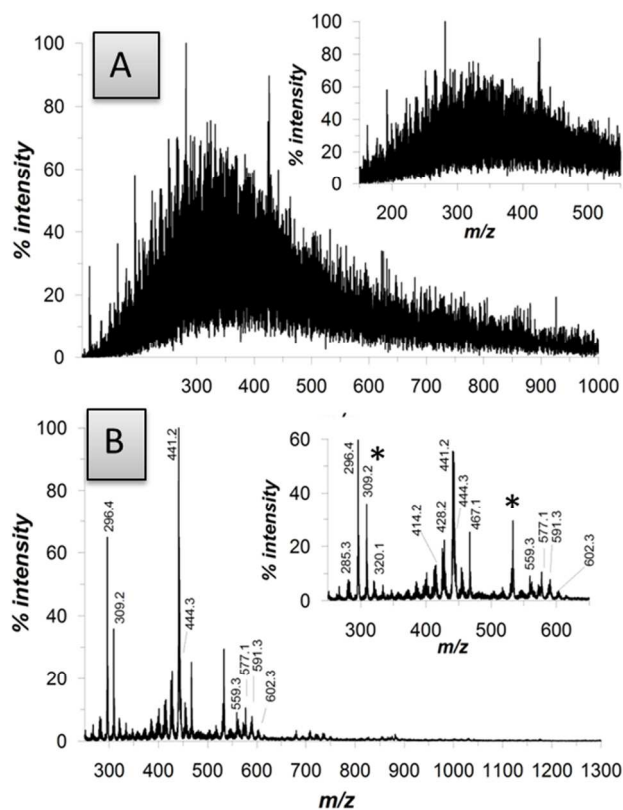


**Figure 3.** MALDI-MS spectra of eumelanin thin films on a standard MALDI plate. A) dopa melanin prepared by alkaline autoxidation.<sup>22</sup> B) DHI melanin prepared by the AISSP methodology. Asterisks denote impurities. See Figure S2 of SI for further details on structural identification

Apparently, ammonia is not incorporated into the chemical structure of the DHI polymer. Both structural integrity (i.e. preservation of indole units and avoiding aromatic ring fission<sup>29</sup>) and control of polymerization can be attributed to the specific constraints and the lack of water associated with the solid state conditions limiting water and/or hydroperoxy anion induced oxidative cleavage of indole units<sup>29</sup> and uncontrolled oligomer chain growth.

Preformed eumelanins are conversely shown by mass spectrometry to be highly heterogeneous as a consequence of disordered polymerization of different units, higher molecular weight dispersion and extensive post-synthetic degradation under the solution conditions of the polymerization processes.

From the technological viewpoint, AISSP thin films proved to be more adhesive (over 3 days in aqueous media without detectable detachment) and smooth. By contrast, films obtained by the previous techniques exhibited marked surface roughness<sup>38</sup> and, most importantly, could be easily detached from the supporting surface by an aqueous medium (not shown). Such worse features can be attributed to the generation of a range of morphologies and to degradative fission of structural units of preformed eumelanins during the harsh synthetic process, decreasing adhesive functionalities in the biopolymer. Indeed low adhesion and tendency to detach on water exposition was also observed with smooth film obtained from dopa according to reported procedure<sup>28</sup> know to provide very smooth surfaces. This was expected, again, on the base of the structural modification

induced by aqueous alkaline treatment and the associated backbone fragmentation and carboxyl groups generation with consequent loss in adhesion to water resistance.

Finally avoiding water and polar solvents in the film fabrication combined with the pigments backbone structural integrity preservation, also allowed to virtually eliminate the known morphological modifications associated with prolonged electrical biasing.<sup>41</sup>

### Effect of Sample Hydration on film electrical properties

As experimentally demonstrated in several works reported in the recent past, the electrical properties of eumelanin films or pellets are largely dominated by the material hydration state.<sup>7, 12</sup>

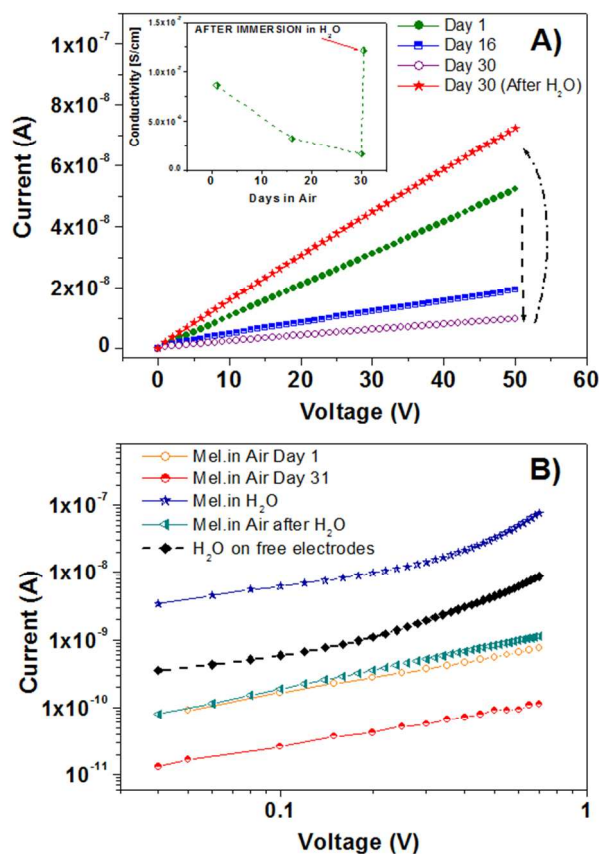


**Figure 4.** (A) Current-Voltage curves for DHI melanin thin films on  $\text{Si}^{++}/\text{SiO}_2/\text{Au}$  substrates recorded after prolonged intervals of storage in air and after the rehydration procedure. In the inset, the related conductivity behavior extracted from IV curves. (B) IV curves measured by sweeping  $V_{\text{DS}}$  voltage from 0 and 0.7 V in different environmental conditions.

Independently on the physical origins, the possibility to exploit such a hydration dependence in the development of eumelanin-based devices appears quite appealing in technological terms and, undoubtedly, worth of further investigation.

In our work, the electrical tests were conducted for DHI melanin thin films deposited on multilayer structures composed of a thick (500  $\mu\text{m}$ ) highly doped ( $\text{Si}^{++}$ ) substrate, a 200 thin  $\text{SiO}_2$  insulating barrier and gold pre-patterned electrodes with interdigitated layout (see Figure S5 A, B of SI). These

Si<sup>++</sup>/SiO<sub>2</sub>/Au structures were considered to investigate the possibility to further modulate the charge transport through eumelanin channels connecting the gold electrodes (source-drain contacts) by applying a gate voltage ( $V_G$ ) to the Si<sup>++</sup> substrate, as commonly done in the basic field-effect transistors (FET). Our measurements, however, indicated clearly the lack of any detectable field-effect response and, hence, the current  $I_{DS}$  hereafter discussed is referred to the basic condition with  $V_G=0V$ .

$I_{DS}$  curves were recorded by sweeping the related  $V_{DS}$  voltage first between 0 and 50 V and then in the backward direction (from 50 to 0 V), with the aim to highlight the presence of hysteresis phenomena. The exemplificative measurement reported in Figure S5 C confirms the presence of a hysteretic behavior with the  $I_{DS}$  values measured in the backward scan being lower than those measured in the forward cycle (clockwise hysteresis). This phenomenon is quite typical of electrically-active materials characterized by poor structural order and gives indications of the occurrence of charge trapping phenomena.

For eumelanin layers, in any case, this effect should be associated also to the presence of proton space charge accumulation effects in the regions close to the electrodes.

This specific feature will be discussed in detail elsewhere, where a set of dynamic electrical measurements will be reported. Here, indeed, the attention was basically focused on the general capability of AISSP-deposited eumelanin films to carry electrical charges. In this regard, Figure 4A reports the  $I_{DS}$  curves measured only during the forward  $V_{DS}$  scan for a sample stored in air within a prolonged period.

From this plot, it is possible to appreciate that the measurements carried out on freshly prepared moisture-equilibrated films exhibited a well-defined ohmic behavior (i.e.  $I_{DS}$  is a linear function of  $V_{DS}$ ) with a conductivity ( $\sigma$ ) value of about  $10^{-7}$  S/cm.

The conducting properties of a pristine eumelanin film were also assessed under the application of continuously repeated IV measurements (Figure S6 of SI). Under this condition, the current flow between the two gold electrodes displayed only a limited (by few percents) decrease over time. This effect should be basically ascribed to the same charge trapping processes invoked above to justify the hysteretic behavior of these channels. It is to mention, however, that all the repeated IV curves preserve the basic ohmic response.

On the other hand, Figure 4A shows that, after a prolonged (30 days) standing in air, a gradual drop by about one order of magnitude in conductivity of the same film occurred. Apparently, the  $\sigma$  lowering was related to the drying process of eumelanin films during the storage in air. In order to confirm this conclusion, eumelanin channels were re-hydrated by covering them with de-ionized water which was left to evaporate during 30 minutes. A final drying with nitrogen gas was carried out to complete the procedure.

As shown, the subsequent IV curve recorded in air confirmed the eumelanin channel capability to recover completely the initial conductivity state. In particular, for these films, several desiccation-hydration cycles (not shown) could be performed stating the fully reversible character of the charge doping/doping process.

After the electrical characterization in air, specific measurements were carried out keeping the eumelanin channels directly immersed in water. In this case, IV curves were recorded by sweeping  $V_{DS}$  voltages between 0 and 0.7 V in order to

minimize the occurrence of electrical currents related to the water electrolysis effect.

As reported in Figure 4B, the IV curve measured for the eumelanin film covered by water displayed considerably higher values than those of the corresponding measurements recorded in air at different times (namely, at different hydration conditions). Moreover, the semi-log plot allows clarifying that the electrical current flowing through the water-covered eumelanin channel exceeds by about one order of magnitude that flowing between two free gold electrodes immersed in the same amount of de-ionized water.

### Investigation of Film Biocompatibility

In a final series of experiments, we investigated the biocompatibility of the DHI melanin films for potential use as bio-interface for stem cell (Murine Embryonic Stem Cell - ESC) growth. The only previous paper in the field reported the ability of thin films from commercial eumelanin to enhance Schwann cell growth and neurite extension compared to collagen films growth,<sup>42</sup>

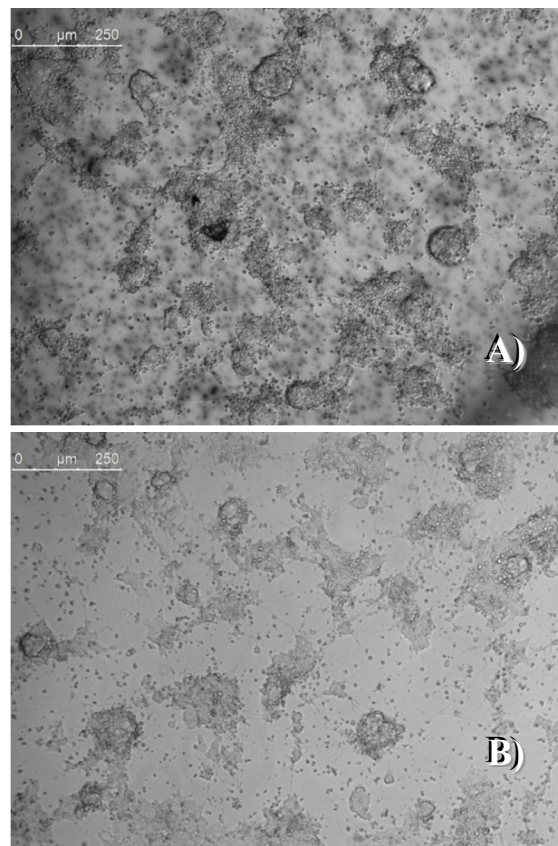


**Figure 5.** Phase contrast image of ESC colonies three days after seeding on dishes coated with melanin coated dishes or gelatin. Stem cells grown on DHI melanin film (upper image: A) and on a Petri gelatin-coated plate as a control (lower image: B). Scale bars: 250 $\mu$ m.

The only previous paper in the field reported the ability of thin films from commercial eumelanin to enhance Schwann cell growth and neurite extension compared to collagen films growth,<sup>42</sup> but the the compatibility with stem cell<sup>43</sup> growth has not yet been reported. This cell population is of particular interest

for tissue engineering application and is under scrutiny for compatibility with classical electro-active materials.<sup>44</sup>

In a series of experiments we addressed the survival and proliferation of undifferentiated ESCs grown on eumelanin films, the preservation of ESC morphology and the occurrence of differentiation.

To assess the ability of eumelanin to support the survival of ESCs, undifferentiated ESCs were trypsinized into a single-cell suspension and  $6 \times 10^4$  cells/cm<sup>2</sup> were plated on 100 mm melanin-coated dish in ESC medium. The medium was changed every day for three days. As shown in Figure 5 eumelanin coating supported adhesion and colony formation of ESCs. ESCs proliferation was evaluated by counting cells after trypsinization and dissociation at 2 and 4 days in colonies plated on dishes coated with eumelanin or with gelatin (as control). As reported in Figure S7 of SI the growth curves of ESCs plated on eumelanin showed a trend comparable with the same cells plated on gelatin indicating that eumelanin does support ESC proliferation.

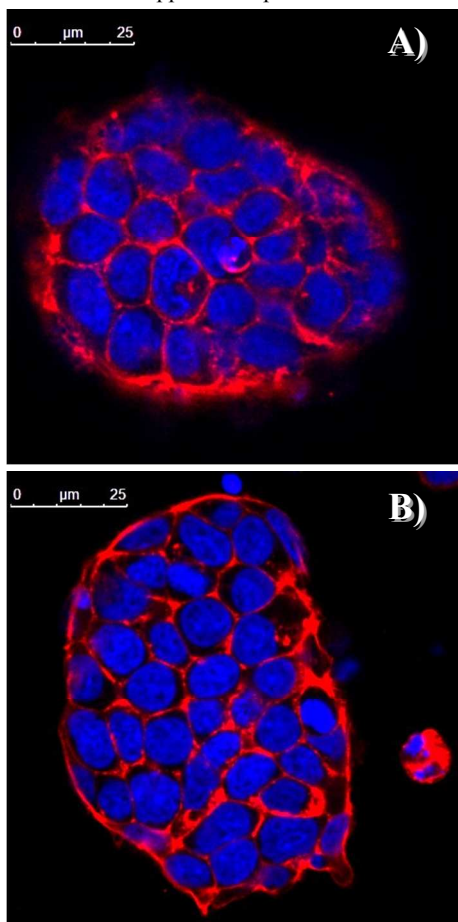


**Figure 6.** Confocal analysis of undifferentiated ESCs grown for 2 days on (A) melanin or (B) gelatin-coated plates and stained with TRITC-labeled phalloidin that binds to F-actin. Nuclei were counterstained with DRQ5. Scale bars: 25 μm. For single channels see Figure S8 of SI.

We also verified eumelanin does not impair ESC morphology by staining F-actin. Figure 6 shows that the structural arrangement of ESCs grown on eumelanin is indistinguishable from those conventionally grown on gelatin. To confirm that the presence of healthy colonies highlighted by the morphological

analysis corresponds to an absence of abnormal cell death we have analyzed the level of active caspase-3, an apoptosis hallmark. As shown in Figure 7, western blot analysis revealed that there is no accumulation of cleaved caspase-3 to the detriment of the uncleaved one that is normally present in healthy cells.

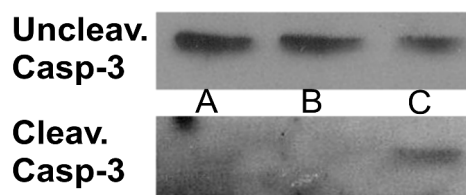


**Figure 7.** Western blot analysis of uncleaved and cleaved caspase-3. ESCs were grown on (A) gelatin or on (B) melanin-coated dishes and after 48 hours were collected. The positive control (C) are ESCs exposed to 15Gy of X rays to induce apoptosis. See Figure S9 for bar graphs depicting the densitometric analysis.

Since we plan to exploit eumelanin films not only to support ESCs grown but also to apply, in future, these substrates to direct the differentiation of pluripotent stem cells into a specific cell fate such as specific neuronal-subpopulations, (i.e. dopaminergic neurons, motoneurons, etc.) we have tested the ability of melanin to allow the neuron formation from undifferentiated ESCs.

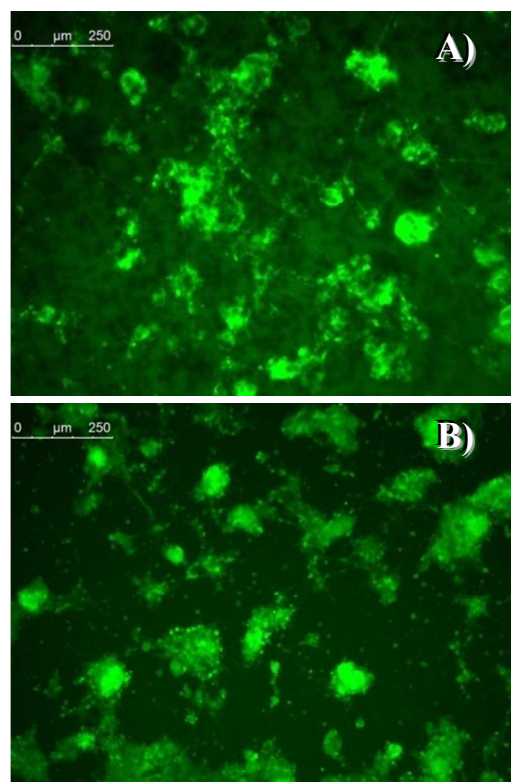


**Figure 8.** Fluorescent live inspection of  $\alpha 1$ -tubulin-GFP ESCs differentiated for 4 days into neuronal lineage on (A) melanin or (B) gelatin-coated plates. The presence of GFP indicated the formation of neuronal precursors. The presence of mature neurons is indicated by the GFP signal in the neuritis. Scale bars: 250 μm.

To this aim, we have used a reporter cell line bearing Green Fluorescent Protein (GFP) under the control of  $\alpha$ 1-tubulin promoter<sup>45</sup>. Thus, the GFP is expressed only when the ESCs differentiate into neuronal precursor or mature neurons. We have employed two differentiation protocol to verify the versatility of melanin film.

In the first protocol, we have allowed neuronal differentiation of ESCs by plating them on gelatin or melanin at low density in a chemically defined medium (see Materials and Methods and reference<sup>46</sup>). As shown in Figure 8, after 4 days of differentiation we have found that the differentiation yield reached on eumelanin is comparable to that on gelatin. The presence of both neural precursors and mature neurons with their axonal extensions is visible in both conditions.

In the second differentiation method we have induced the formation of serum free embryoid bodies in suspension SFEBS, (see Materials and Methods and reference<sup>47</sup>) that allow the formation of neuronal precursors and then, upon adhesion on an appropriate substrate, the formation of mature neurons. Figure S10 of SI shows that melanin supports the development of mature neurons from neural precursors derived from SFEBS after 11 days of differentiation.

All together these results suggest that eumelanin is able not only to support normal growth of ESCs without impairing proliferation and survival but, importantly, this substrate is able to allow the formation of neuronal precursors and neurons starting from undifferentiated ESCs (first differentiation method) and the development of mature neurons from already established neural precursors (second differentiation method).

## Conclusion.

In light of chemical properties of 5,6-dihydroxyindole, chiefly its high oxidizability, we speculated on the possibility to access eumelanin films circumventing typical difficulties connected to the intractable nature of this pigment and, at the same time, gain a chemical control of the pigment backbone.

We have reported herein high quality eumelanin thin films displaying appealing features, such as reversible conductivity by controlled hydration-dehydration steps, excellent biocompatibility with stem cells, water resistant adhesion, for bioelectronic applications.

The morphology and the chemical uniformity and nature of the eumelanin films may be expected to play a key role in allowing cell cultures. Stem cells are highly sensitive to environment and their adhesion and healthy growth on eumelanin films here reported denotes not only generic biocompatibility of the films but also their identification as safe substrate not inducing suicide and capable of supporting differentiation up to 11 days.

Important advantages of the AISSP procedure with respect to previously reported protocols include: 1) efficient chemical control on structural disorder and film morphology, due to the facile deposition of the soluble DHI monomer opening the way to more efficient chemical manipulation and tailoring; 2) robustness and strong adhesion of the resulting film to a variety of substrates, from glass to silicon and plastic polymers; 3) the lack of artifacts associated with post synthetic work-up procedures; 4) synthetic versatility for controlled polymerization and copolymerization with other co-substrates or for engineering wafer architectures; 5) low environmental impact due to the solvent-free, oxygen-based protocol. Very significantly, the AISSP procedure is of general relevance, being applicable to any easily oxidizable and filmable polyphenolic substrate.

Moreover, in this work, AISSP technique was applied on various types of substrates. In particular, eumelanin films were deposited on quartz (see Figures S1 and S11 of SI), SiO<sub>2</sub>, and ITO (Indium-Tin Oxide) exhibiting substantially the same structural and morphological properties. In principle, the AISSP technique has no limitation with respect to the substrate. Indeed eumelanin coating via the AISSP technique is achievable for any substrate (organic as well as inorganic) featuring a low contact angle (below 30°) with a solvent capable to sustain DHI concentration up to 30 mg/ml.

The properties of the eumelanin films described herein may pave the way to the design and implementation of organic electrochemical transistors (OECT)<sup>48, 49</sup> featuring full biocompatibility even with highly sensitive stems cell cultures and capable of translating cellular activity in electrical signals.

## Acknowledgements

This work was supported by a grant from Italian MIUR (PRIN 2010-2011, 010PFLRJR “PROxi” project), by a grant to SP from Ministry of University and Research for the projects: Futuro in Ricerca 2013 (RBF13YZ2Y) and was carried out in the frame of the EuMelaNet program (<http://www.espcr.org/eumelanet>) and the PolyMed project within the FP7-PEOPLE-2013-IRSES frame, PIRSES-GA-2013-612538

## Notes and references

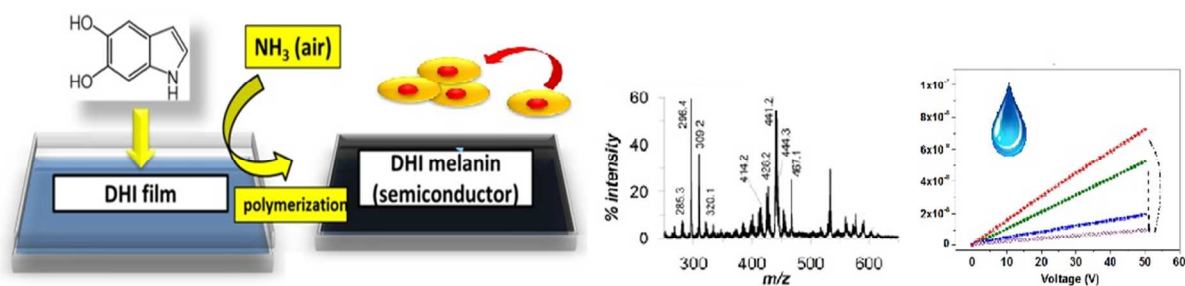
- <sup>a</sup> Department of Chemical Sciences, University of Naples “Federico II” Via Cintia 4, I-80126 Naples, Italy E-mail: [alessandro.pezzella@unina.it](mailto:alessandro.pezzella@unina.it)
- <sup>b</sup> CNR-SPIN and Department of Physics Science, University of Naples Federico II, Naples 80125, Italy
- <sup>c</sup> Department of Molecular medicine and Medical Biotechnology, University of Naples “Federico II”
- <sup>d</sup> Department of Molecular medicine and Medical Biotechnology, University of Naples “Federico II”, 80131 Naples; Ceinge Biotechnologie Avanzate Via Gaetano Salvatore 486, 80145 Naples, Italy
- <sup>e</sup> CNR, Istituto di Ricerche sulla Combustione, Naples, Italy
- † Electronic Supplementary Information (ESI) available: [Detailed experimental methods and film characterization is available]. See DOI: 10.1039/b000000x/
- ‡ Footnotes should appear here. These might include comments relevant to but not central to the matter under discussion, limited experimental and spectral data, and crystallographic data.
1. M. d'Ischia, A. Napolitano, A. Pezzella, P. Meredith and T. Sarna, *Angew Chem Int Edit*, 2009, **48**, 3914-3921.
  2. P. Meredith, C. J. Bettinger, M. Irimia-Vladu, A. B. Mostert and P. E. Schwenn, *Rep Prog Phys*, 2013, **76**, 034501.
  3. M. d'Ischia, K. Wakamatsu, A. Napolitano, S. Briganti, J. C. Garcia-Borron, D. Kovacs, P. Meredith, A. Pezzella, M. Picardo, T. Sarna, J. D. Simon and S. Ito, *Pigment cell & melanoma research*, 2013, **26**, 616-633.
  4. S. Ito and K. Wakamatsu, *J Eur Acad Dermatol*, 2011, **25**, 1369-1380.
  5. J. D. Simon, D. Peles, K. Wakamatsu and S. Ito, *Pigment cell & melanoma research*, 2009, **22**, 563-579.
  6. J. McGinness, P. Corry and P. Proctor, *Science*, 1974, **183**, 853-855.

7. A. B. Mostert, B. J. Powell, F. L. Pratt, G. R. Hanson, T. Sarna, I. R. Gentle and P. Meredith, *Proceedings of the National Academy of Sciences of the United States of America*, 2012, **109**, 8943-8947.
8. J. Wunsche, F. Cicoira, C. F. O. Graeff and C. Santato, *Journal of Materials Chemistry B*, 2013, **1**, 3836-3842.
9. P. Meredith and T. Sarna, *Pigm Cell Res*, 2006, **19**, 572-594.
10. A. Pezzella, A. Iadonisi, S. Valerio, L. Panzella, A. Napolitano, M. Adinolfi and M. d'Ischia, *J Am Chem Soc*, 2009, **131**, 15270-15275.
11. L. Panzella, G. Gentile, G. D'Errico, N. F. Della Vecchia, M. E. Errico, A. Napolitano, C. Carfagna and M. d'Ischia, *Angew Chem Int Ed Engl*, 2013, **52**, 12684-12687.
12. A. B. Mostert, G. R. Hanson, T. Sarna, I. R. Gentle, B. J. Powell and P. Meredith, *The journal of physical chemistry. B*, 2013, **117**, 4965-4972.
13. M. Gauden, A. Pezzella, L. Panzella, M. T. Neves-Petersen, E. Skovsen, S. B. Petersen, K. M. Mullen, A. Napolitano, M. d'Ischia and V. Sundstrom, *J Am Chem Soc*, 2008, **130**, 17038-17043.
14. A. Corani, A. Huijser, A. Iadonisi, A. Pezzella, V. Sundstrom and M. d'Ischia, *The journal of physical chemistry. B*, 2012, **116**, 13151-13158.
15. M. L. Tran, B. J. Powell and P. Meredith, *Biophys J*, 2006, **90**, 743-752.
16. L. Ascione, A. Pezzella, V. Ambrogio, C. Carfagna and M. d'Ischia, *Photochemistry and photobiology*, 2013, **89**, 314-318.
17. A. Pezzella, O. Crescenzi, L. Panzella, A. Napolitano, E. J. Land, V. Barone and M. d'Ischia, *J Am Chem Soc*, 2013, **135**, 12142-12149.
18. M. Jastrzebska, A. Kocot, J. K. Vij, J. Zalewska-Rejdek and T. Witek, *J Mol Struct*, 2002, **606**, 205-210.
19. P. J. Goncalves, O. Baffa and C. F. O. Graeff, *J Appl Phys*, 2006, **99**.
20. N. F. Della Vecchia, R. Avolio, M. Alfe, M. E. Errico, A. Napolitano and M. d'Ischia, *Adv Funct Mater*, 2013, **23**, 1331-1340.
21. J. Liebscher, R. Mrowczynski, H. A. Scheidt, C. Filip, N. D. Hadade, R. Turcu, A. Bende and S. Beck, *Langmuir : the ACS journal of surfaces and colloids*, 2013, **29**, 10539-10548.
22. C. T. Chen, V. Ball, J. J. de Almeida Gracio, M. K. Singh, V. Toniazzo, D. Ruch and M. J. Buehler, *ACS nano*, 2013, **7**, 1524-1532.
23. M. Ambrico, P. F. Ambrico, A. Cardone, T. Ligonzo, S. R. Cicco, R. Di Mundo, V. Augelli and G. M. Farinola, *Adv Mater*, 2011, **23**, 3332-+.
24. M. Ambrico, P. F. Ambrico, A. Cardone, N. F. Della Vecchia, T. Ligonzo, S. R. Cicco, M. M. Talamo, A. Napolitano, V. Augelli, G. M. Farinola and M. d'Ischia, *J Mater Chem C*, 2013, **1**, 1018-1028.
25. M. Ambrico, P. F. Ambrico, A. Cardone, S. R. Cicco, F. Palumbo, T. Ligonzo, R. Di Mundo, V. Petta, V. Augelli, P. Favia and G. M. Farinola, *J Mater Chem C*, 2014, **2**, 573-582.
26. M. Abbas, M. Ali, S. K. Shah, F. D'Amico, P. Postorino, S. Mangialardo, M. Cestelli Guidi, A. Cricenti and R. Gunnella, *The journal of physical chemistry. B*, 2011, **115**, 11199-11207.
27. A. B. Mostert, K. J. Davy, J. L. Ruggles, B. J. Powell, I. R. Gentle and P. Meredith, *Langmuir : the ACS journal of surfaces and colloids*, 2010, **26**, 412-416.
28. J. P. Bothma, J. de Boor, U. Divakar, P. E. Schwenn and P. Meredith, *Adv Mater*, 2008, **20**, 3539-+.
29. A. Napolitano, A. Pezzella, M. R. Vincensi and G. Prota, *Tetrahedron*, 1995, **51**, 5913-5920.
30. R. Noriega, J. Rivnay, K. Vandewal, F. P. V. Koch, N. Stingelin, P. Smith, M. F. Toney and A. Salleo, *Nat Mater*, 2013, **12**, 1037-1043.
31. A. Pezzella, L. Panzella, A. Natangelo, M. Arzillo, A. Napolitano and M. d'Ischia, *J Org Chem*, 2007, **72**, 9225-9230.
32. A. Pezzella, L. Panzella, O. Crescenzi, A. Napolitano, S. Navaratman, R. Edge, E. J. Land, V. Barone and M. d'Ischia, *J Am Chem Soc*, 2006, **128**, 15490-15498.
33. M. D'Ischia, A. Napolitano, A. Pezzella, E. J. Land, C. A. Ramsden and P. A. Riley, *Adv Heterocycl Chem*, 2005, **89**, 1-63.
34. L. Panzella, A. Pezzella, A. Napolitano and M. d'Ischia, *Org Lett*, 2007, **9**, 1411-1414.
35. S. Reale, M. Crucianelli, A. Pezzella, M. d'Ischia and F. De Angelis, *Journal of mass spectrometry : JMS*, 2012, **47**, 49-53.
36. M. Arzillo, G. Mangiapia, A. Pezzella, R. K. Heenan, A. Radulescu, L. Paduano and M. d'Ischia, *Biomacromolecules*, 2012, **13**, 2379-2390.
37. G. Tarabella, A. Pezzella, A. Romeo, P. D'Angelo, N. Coppede, M. Calicchio, M. d'Ischia, R. Mosca and S. Iannotta, *Journal of Materials Chemistry B*, 2013, **1**, 3843-3849.
38. F. Bloisi, A. Pezzella, M. Barra, M. Alfe, F. Chiarella, A. Cassinese and L. Vicari, *Appl Phys a-Mater*, 2011, **105**, 619-627.
39. F. Bloisi, A. Pezzella, M. Barra, F. Chiarella, A. Cassinese and L. Vicari, *J Appl Phys*, 2011, **110**.
40. G. Prota, *Med Res Rev*, 1988, **8**, 525-556.
41. J. Wunsche, L. Cardenas, F. Rosei, F. Cicoira, R. Gauvin, C. F. O. Graeff, S. Poulin, A. Pezzella and C. Santato, *Adv Funct Mater*, 2013, **23**, 5591-5598.
42. C. J. Bettinger, P. P. Bruggeman, A. Misra, J. T. Borenstein and R. Langer, *Biomaterials*, 2009, **30**, 3050-3057.
43. M. R. Alison, R. Poulos, S. Forbes and N. A. Wright, *The Journal of pathology*, 2002, **197**, 419-423.
44. I. N. Wang, J. T. Robinson, G. Do, G. Hong, D. R. Gould, H. Dai and P. C. Yang, *Small*, 2014, **10**, 1479-1484.
45. S. Parisi, F. Passaro, L. Aloia, I. Manabe, R. Nagai, L. Pastore and T. Russo, *Journal of cell science*, 2008, **121**, 2629-2634.
46. Q. L. Ying, M. Stavridis, D. Griffiths, M. Li and A. Smith, *Nature biotechnology*, 2003, **21**, 183-186.
47. S. Parisi, M. Battista, A. Musto, A. Navarra, C. Tarantino and T. Russo, *FASEB journal : official publication of the Federation of American Societies for Experimental Biology*, 2012, **26**, 3957-3968.
48. D. Khodagholy, J. Rivnay, M. Sessolo, M. Gurfinkel, P. Leleux, L. H. Jimison, E. Stavrinidou, T. Herve, S. Sanaur, R. M. Owens and G. G. Malliaras, *Nat Commun*, 2013, **4**.
49. M. Bongo, O. Winther-Jensen, S. Himmelberger, X. Strakosas, M. Ramuz, A. Hama, E. Stavrinidou, G. G. Malliaras, A. Salleo, B. Winther-Jensen and R. M. Owens, *Journal of Materials Chemistry B*, 2013, **1**, 3860-3867.

## Graphical Abstract

### Stem Cell-Compatible Eumelanin Biointerface by Chemically-Controlled Solid State Polymerization

Alessandro Pezzella, Mario Barra, Angelica Navarra, Michela Alfè, Paola Manini, Silvia Parisi, Antonio Cassinese, Marco d'Ischia



High quality eumelanin thin film featuring efficient reversibility of the water induced conductivity switch and a high biocompatibility was obtained. Key feature of the new biointerface is a remarkable chemical control over eumelanin structural integrity and molecular diversity via ammonia-induced solid state polymerization of a 5,6-dihydroxyindole thin film.